

Measuring the true quality factor of an ultrafast photonic microcavity: homogeneous versus inhomogeneous broadening

Alex Hartsuiker*

Center for Nanophotonics, FOM Institute for Atomic and Molecular Physics (AMOLF), Kruislaan 407, 1098 SJ Amsterdam, The Netherlands

Allard P. Mosk

Complex Photonic Systems (COPS), MESA+ Institute for Nanotechnology, University of Twente, The Netherlands

Julien Claudon and Jean-Michel Gérard

CEA-CNRS, "Nanophysics and Semiconductors" joint laboratory,
CEA/INAC/SP2M, 17 rue des Martyrs, 38054 Grenoble Cedex 9, France

Willem L. Vos

Center for Nanophotonics, FOM Institute for Atomic and Molecular Physics (AMOLF),
Kruislaan 407, 1098 SJ Amsterdam, The Netherlands and

Complex Photonic Systems (COPS), MESA+ Institute for Nanotechnology, University of Twente, The Netherlands

(Dated: December 12, 2021, version 1)

We have measured time-resolved the photon storage time and the quality factor of an ultrafast photonic cavity using an autocorrelator. The cavity consists of a λ -thick GaAs layer sandwiched between GaAs/AlAs distributed Bragg reflectors and resonates at 985 nm wavelength. The inverse relative linewidth measured with white light reflectivity is 830, while the quality factor obtained from the time resolved measurements is 1500. The photon storage time in the cavity is 0.78 ps. We show that the difference between the quality factor and the inverse relative linewidth results from inhomogeneous broadening of the microcavity resonance due to a spatial gradient in the cavity layer.

PACS numbers:

INTRODUCTION

Since light is extremely elusive there is a great interest to store photons in a small volume for a certain time. Storage of photons in an applicable way can be achieved using solid state cavities. Tanabe *et al.* used cavities to create large pulse delays with small group velocities by storing light in a cavity inside a 2D photonic crystal slab [1, 2]. Another application where storage of light in a cavity plays a crucial role is changing the color of light as was studied by Preble *et al.* [3]. Ultimately, with a microcavity the strong coupling regime of cavity quantum electro dynamics can be entered [4, 5]. In the strong coupling regime a cavity and a two level system together form a new set of states. Normal-mode splitting of a coupled exciton-photon mode was observed in a planar microcavity [6]. Other interesting experiments have been performed on planar cavities, e.g Bose-Einstein condensation of exciton polaritons [7] and the investigation of the limitations of a scanning Fabry-Pérot interferometer [8].

An important characteristic parameter of a cavity resonance is the storage time of light τ_{cav} . The storage time is defined by the response of the cavity resonance to a Dirac pulse. Excitation of the electromagnetic field in a cavity was studied in [9]. The response to the Dirac pulse is given by an exponential decay of the intensity $I(t)$ in the cavity resonance [10]:

$$I(t) = I_0 e^{-t/\tau_{cav}}, \quad (1)$$

with I_0 the initial intensity that the pulse stores in the cavity. However, in more complex cavities the behavior of the cavity

can be very different from the single exponential case [11]. To compare cavities independent of their resonance frequencies ω_0 , the widely used figure of merit is the resonance quality factor Q , which is defined as:

$$Q \equiv \tau_{cav} \omega_0. \quad (2)$$

Physically, the quality factor is proportional to the ratio between the total energy stored and the energy lost per cycle. At optical frequencies a cavity with a feasible high quality factor of $Q = 10^6$ is relatively slow with a response time in the order of nanoseconds. A cavity with a moderate quality factor $Q = 1000$, however, is fast with a response time of picoseconds. The picosecond timescale allows ultrafast access and storage of light in the cavities.

A common procedure to estimate the quality factor of a cavity is to measure a transmission or reflectivity spectrum and extract Q from the relative linewidth of the cavity resonance [3, 4, 5, 12, 13, 14, 15]. For a single resonance without dephasing, one can use the Wiener-Khinchine theorem, which relates the field autocorrelate to the intensity spectrum, to obtain

$$Q = \frac{\omega_0}{\Delta\omega}. \quad (3)$$

However, if there is significant dephasing, e.g. due to inhomogeneous broadening or thermal noise, $\Delta\omega$ will in general be larger and $Q > \omega_0/\Delta\omega$.

From many resonating systems in condensed matter and solid state physics, it is known that besides homogeneous

broadening there is also the possibility of inhomogeneous broadening of a resonance [16, 17]. In the case of an ensemble of resonators inhomogeneous broadening of a resonance results from inhomogeneities in the resonance frequency. If the resonance frequency is different for each resonator the linewidth of the ensemble is broader than the linewidth of a single resonator and the ensemble linewidth is typically determined by the distribution of resonance frequencies. In the case of inhomogeneous broadening the linewidth will only give a lower boundary for the range of possible Q values. The true quality factor must in this case be determined from dynamic measurements.

A dynamic measurement to determine the quality factor is a cavity ring down experiment as was treated in [18]. In this case a cavity is excited by a pulse and the intensity emitted from the cavity is measured as a function of time. In the case of storage times in the order of nanoseconds and very high quality factors ($Q = 10^6$) time correlated single photon counting can be used to determine the storage time [1]. In our case of ultrafast cavities that decay on a ps timescale with moderate quality factor ($Q = 1000$), an intensity autocorrelation function is the method of choice for determining the quality factor.

The normalized correlation function that is measured is an intensity autocorrelation function G^2 , which is given by [19]

$$G^2(\tau) = \frac{\langle I(t)I(t-\tau) \rangle}{I_0^2}, \quad (4)$$

where τ is the delay time between the pulses from each of the interferometer branches, I_0^2 is equal to maximum value of the unnormalized autocorrelation value, and $I(t)$ is the time dependent intensity. There is no phase in equation 4, which means that this is the proper autocorrelation function, also in case of dephasing. The autocorrelate has its maximum at delay $\tau = 0$, when the pulses in the two branches of the Michelson interferometer overlap. For example the autocorrelate of a Gaussian pulse is given by a Gaussian shape, where the width of the input pulse τ_{ip} and the autocorrelate are related as $\tau_{ac} = \sqrt{2}\tau_{ip}$. From the autocorrelate of a pulse stored in the cavity resonance, the storage time can be found from the full width at half maximum τ_{FWHM} of G^2 , with $\tau_{cav} = 0.63\tau_{FWHM}$.

EXPERIMENTAL

Our structure is a planar cavity that consists of a GaAs λ -thick layer (277 nm thick), sandwiched between two Bragg stacks. One Bragg stack consists of 12 and the other Bragg stack consists of 16 pairs of $\lambda/4$ -thick layers of nominally pure GaAs or AlAs. The same structure was studied in Ref. [15]. The sample was grown at CEA in Grenoble by means of molecular beam epitaxy at 550°C [20]. For experiments outside the present scope the sample was doped with 10^{10}cm^{-2} InGaAs/GaAs quantum dots, which hardly influence our ex-

periment [28]. There is a spatial gradient in the cavity thickness of $\frac{\delta d}{\delta x} = 5.64 \text{ nm/mm}$ [21]. The spatial gradient results in a position dependent resonance frequency. In our measurements we average the transmitted intensity over the area of the focal spot. The different resonance frequencies cause the resonance to broaden inhomogeneously.

White-light reflectivity and transmission were measured with a broadband white-light spectrometer setup with a spectral resolution of about $\Delta\lambda = 0.2 \text{ nm}$ [22]. The transmission spectrum was measured with a collimated beam with a diameter of 2 mm. The reflectivity spectrum was measured with a glass objective with a numerical aperture $\text{NA} = 0.05$ and a focus diameter of 100 μm . The reflectance spectrum of a gold mirror was used as a reference.

For pulse transmission and the intensity autocorrelate, we used a Titanium Sapphire laser that emits $\tau_{ip} = 0.115 \text{ ps}$ pulses at $\lambda = 800 \text{ nm}$ at a repetition rate of 1 kHz (Hurricane, Spectra Physics). The laser drives an optical parametric amplifier (OPA, Topas 800-fs, Light Conversion), which generates the pulses used to probe the photonic cavity. The center wavelength of the OPA pulses can be tuned between 450 nm and 2400 nm. We used a fiber optic spectrometer (USB2000, Ocean Optics) to measure transmission spectra of the femtosecond pulses. We measured with an unfocused collimated beam with a spot diameter of 2 mm, and a numerical aperture $\text{NA} = 10^{-4}$. The intensity autocorrelation function was measured using a Pulse Check autocorrelator (APE GmbH). The autocorrelator consists of a Michelson interferometer with a scanned delay path and a nonlinear crystal that generates second harmonic light. The autocorrelator has a maximum range of 15 ps with a resolution of 1 fs. We used the same beam parameters as in transmission. The intensity on the sample is 100 kWcm^{-2} , sufficiently low to avoid non-linear effects.

Simulations were performed with the finite-difference time-domain (FDTD) method using a freely available software package with subpixel smoothing for increased accuracy [23].

EXPERIMENTAL RESULTS

In figure 1 A we show the reflection and transmission spectra of the planar cavity. A prominent stopband with a reflection of 100 % and a transmission of 0 % is visible. Outside the stopband a Fabry-Pérot fringe pattern is visible, while inside the stopband a narrow trough in reflection and a narrow peak in transmission mark the position of the cavity resonance. An effect of the spatial gradient in the cavity thickness is visible in the spectra in figure 1 B: The frequencies of the peak and trough, which are measured at different sample position, differ slightly. Reflectivity and transmission measurements on the same spot are shown as an inset in figure 1 B. The trough and the peak are clearly at the same wavelength as expected.

The solid line in figures 1 A and 1 B represents a transfer matrix (TM) calculation, with fixed complex input parameters n_{GaAs} [24] and n_{AlAs} [25]. The thickness of the $\lambda/4$ layers ($d_{\text{GaAs}} = 70.2 \text{ nm}$ and $d_{\text{AlAs}} = 83.2 \text{ nm}$) and the thickness of

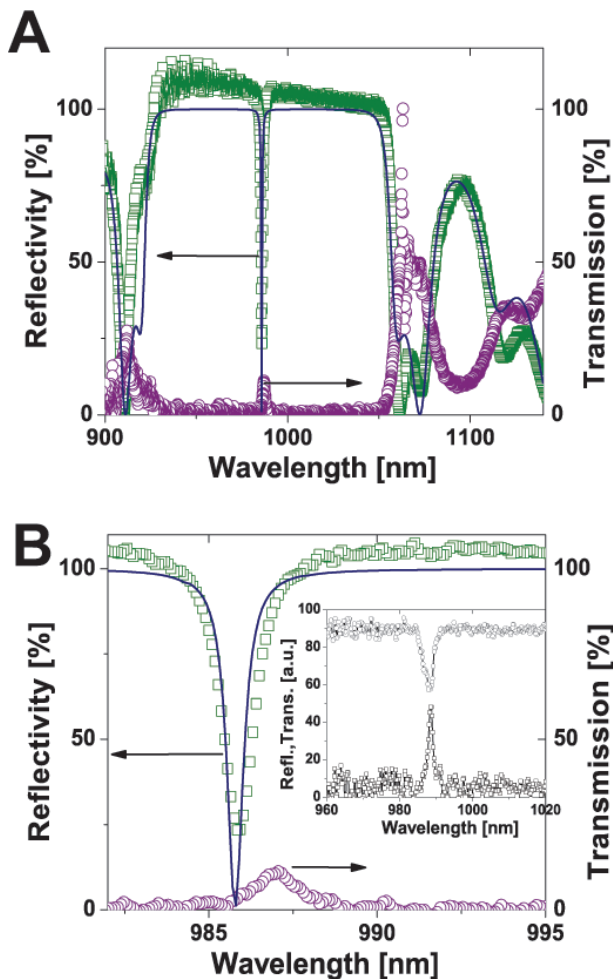


FIG. 1: (A) Linear reflectivity and transmission spectrum of the GaAs/AlAs microcavity. The solid line represents the fit with a Transfer Matrix (TM) model. A stop band is apparent in both reflection and transmission; the trough in the reflectivity spectrum and the peak in the transmission spectrum reveal the presence of the cavity. (B) Zoom-in of (A). From the linewidth of the trough and peak, an inverse relative linewidth of 830 was found in reflection and transmission. The resonance is slightly shifted between the transmission and reflection measurement due to realignment of the sample between the measurements. The inset in B shows a reflection and a transmission spectrum, measured at the same position. Here the trough and peak are clearly at the same wavelength.

the cavity ($d_{cav} = 277$ nm) were obtained by fitting the results of the calculations to the measured spectrum. These values are in agreement with expected values from the fabrication process. The calculation fits well with respect to frequency and amplitude. The reflectivity of the measured stopband is higher than the calculated value of 100 % because of a small systematic error in the gold reference spectrum.

It is apparent from figure 1 B that the calculated linewidth of the cavity resonance is narrower than the measured linewidth. We attribute this discrepancy to inhomogeneous broadening of the measured linewidth, due to the spatial gra-

dient in the cavity layer thickness. With the $100 \mu\text{m}$ diameter spot we average over different positions and therefore over different resonance frequencies. Broadening due to a spread in wavevectors can be neglected since the numerical aperture of the impinging beam was made very small ($NA < 0.05$), as opposed to [15], where a high NA was used. We find that the relative linewidth in both reflection and transmission equals $\frac{\lambda_0}{\Delta\lambda} = 830$, with $\Delta\lambda$ the full width at half maximum (FWHM) and λ_0 the resonance wavelength. The transfer matrix calculation yields an inverse relative linewidth of 1640 ± 100 , about double the value of the inverse linewidth measured with white-light spectroscopy.

We measured the intensity autocorrelation traces to determine the true storage time and Q of the cavity resonance with a time-resolved measurement. Figure 2 shows the autocorrelation traces at values of the center wavelength of the OPA, $\lambda_{OPA} = 930$ nm (A), $\lambda_{OPA} = 985$ nm (B) and $\lambda_{OPA} = 1070$ nm (C). All figures show that the pulses that are transmitted

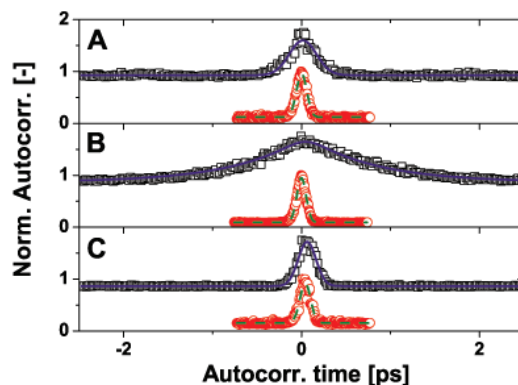


FIG. 2: Normalized intensity autocorrelation traces of pulses transmitted through a planar cavity at different OPA wavelength settings: 930 nm (A), 985 nm (B) and 1070 nm (C). The autocorrelation traces of the input pulses are given by the circles, while the autocorrelation traces of pulses transmitted through the cavity are offset by 0.9 and given by squares. The dashed and solid lines are fits to the autocorrelation traces, without and with sample respectively. The shape of the autocorrelation trace is Gaussian for the pulses from the OPA. The pulses that are on resonance with the cavity show an autocorrelation that agrees very well with the autocorrelation trace from the damped oscillator model (B). The shape of the pulses transmitted through a non-photonic range of the sample remains Gaussian.

through the sample are broader than the input pulses. The width of the input pulses is $\tau_{ip} = 0.115$ ps and the shape Gaussian, which we expect from the specifications of our laser system. The transmitted pulses are broadened by dispersion in the off resonance cases (A) and (C). In the case of figure 2 B the broadening is the result of the storage of the photons in the cavity.

The shape of the autocorrelation trace of the transmitted pulses is Gaussian for pulses transmitted outside the stop

band, as expected. The autocorrelation traces measured on resonance with the cavity (B) are non-Gaussian. This is typical for autocorrelation traces near the cavity resonance, because of the exponential decay of the energy stored in the cavity. The autocorrelation traces calculated with a damped oscillator model is shown in figure (B) and fits the experimental data very well. From the width of the autocorrelation trace on resonance ($\tau_{FWHM} = 1.1$ ps), we conclude that the true storage time of our cavity is $\tau_{cav} = 0.78 \pm 0.05$ ps.

To further analyze the autocorrelation traces we plot the full width at half maximum of the measured autocorrelation traces. The results are shown in figure 3 A as a function of center wavelength of the laser. The width of the autocorrelate

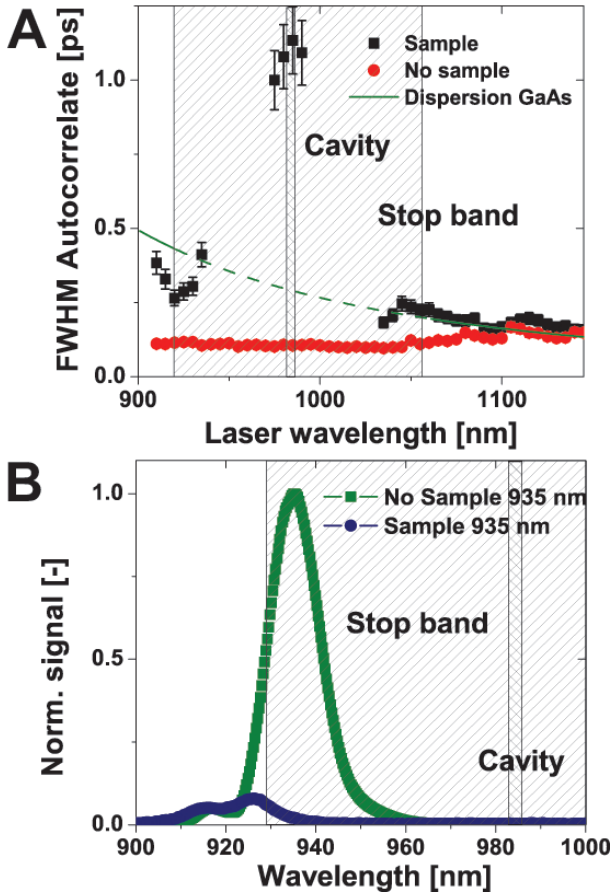


FIG. 3: (A) Pulse width as a function of wavelength setting. The pulses that passed through the sample (squares) are broadened with respect to the input pulses (circles). The solid/dashed line represents the FWHM of a 15 nm spectrally wide input pulse that is transmitted through a 350 μm GaAs wafer that is used as a substrate. (B) Normalized spectrum transmitted through the microcavity, and reference spectra of pulses directly from the OPA. For 935 nm wavelength setting (green squares) the transmitted spectrum consists of the tail of the input spectrum that continues in the region on the blue side of the stop band (blue circles).

of pulses without the sample is $\tau_{ac} = 0.115 \times \sqrt{2}$ ps and essentially independent of laser wavelength, as expected from

the OPA specifications. In the presence of the sample, we observe a more complex dependency on the wavelength, with three regimes: Transmission on resonance, transmission outside the stopband, transmission inside the stopband. Near the cavity resonance the width of the autocorrelate increases drastically to $\tau_{FWHM} = 1.1$ ps. The width of the autocorrelate at the cavity resonance is attributed to the storage of light in the cavity: The storage time of the cavity $\tau_{cav} = 0.78 \pm 0.05$ ps and the quality factor is equal to 1500 ± 100 .

Outside the stopband the pulses are broadened. The width of the autocorrelate outside the stop band is about $0.2 \times \sqrt{2}$ ps. We attribute the broadening outside the stopband region to dispersion in the GaAs substrate. From figure 3A it can be seen that the width of the autocorrelation traces matches well the expected width for a pulse transmitted through a GaAs wafer [26]. The expected width is calculated for a GaAs wafer with a thickness of 350 μm , from the dispersion given by Blake-more [24].

In figure 3 A, we observe datapoints inside the stopband, where a transmission of 0 % is expected. We measure values for the width that are close to the values outside the stopband. The situation in this case is sketched in figure 3 B where we see the transmitted spectrum with and without sample. We observe that the blue part of the spectrum is transmitted, which means that the measured width of the intensity autocorrelate is the value for the blue side of the stopband.

MODELING

To obtain a physical picture of the decay mechanism inside the cavity and to verify what the true Q is, we model the behavior with a damped harmonic oscillator. We furthermore performed FDTD calculations to calculate the Q of the cavity in the ideal case and to check the validity of the harmonic oscillator model [29].

The response of a damped harmonic oscillator with $Q = 1450$ to a Gaussian input pulse with a width of $\tau_{ip} = 0.2$ ps is shown in figure 4, together with the Gaussian input pulse and the cavity response as calculated with FDTD. No dispersion and no absorption was taken into account for the FDTD calculations. In the harmonic oscillator case and in the FDTD case the intensity decays exponentially and with the same rate. Therefore, we conclude that the harmonic oscillator is a suitable model to describe in a simple way the decay of the microcavity. Furthermore the quality factor of the cavity without absorption and dispersion is equal to $Q = 1450 \pm 100$.

With the damped harmonic oscillator model we have calculated the autocorrelates that are shown together with the measured data in figure 5 for a quality factor of the damped harmonic oscillator $Q = 1500$ and Gaussian input pulse with width 0.12 ps. Figure 5 shows a very good agreement between the measured autocorrelation trace and the calculated autocorrelation trace for $Q = 1500$. The autocorrelate obtained from this model has a FWHM of 1.2 ps, which is in very good agreement with the measured value of 1.1 ps.

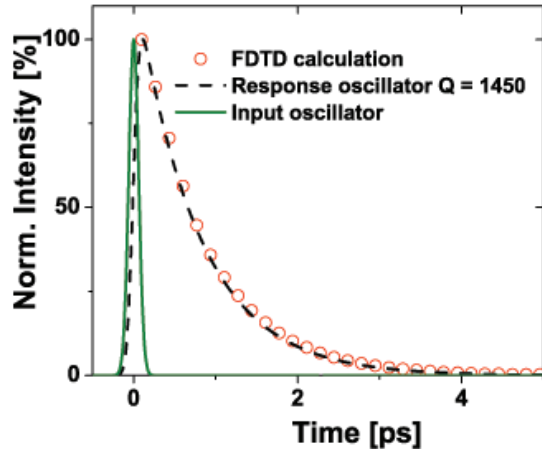


FIG. 4: Response of a damped harmonic oscillator with a quality factor $Q = 1450$ (dashed) to a Gaussian input pulse (solid). The output pulse is the input pulse convoluted with the impulse response of the oscillator. The symbols represent the resulting decay of the intensity in the cavity, as obtained from the FDTD calculation.

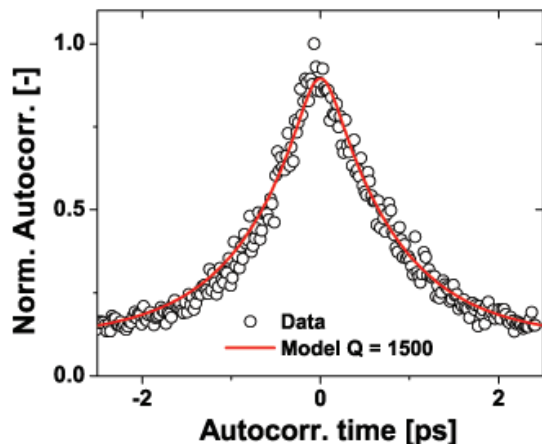


FIG. 5: Autocorrelate of pulse transmitted at the cavity resonance (circles). The solid line represents the result from a simple oscillator model with $Q = 1500$. The input pulse duration is 0.12 ps.

Table I presents the results of the various methods to determine the quality factor presented in this work. We see that the value for the inverse linewidth found from the transfer matrix model agrees well with the value found from the autocorrelator measurement. The slight discrepancy might be attributed to minor irregularities in the structure. We conclude that the quality factor of the cavity is 1500 ± 100 and the storage time of light 0.78 ± 0.05 ps. The inverse linewidth measured in reflection and transmission with white light spectroscopy is much smaller than the value from autocorrelator

TABLE I: Overview of inverse linewidths and cavity lifetimes measured and calculated with presented methods.

	Method	$\frac{\lambda_0}{\Delta\lambda}$	τ_{cav} (ps)
Measurement	Autocorrelator	1500 ± 100	0.78 ± 0.05
	Ref./Trans.	830 ± 50	0.43 ± 0.02
Theory	Transfer Matrix	1640 ± 100	0.93 ± 0.05
	FDTD	1450 ± 100	0.75 ± 0.05

measurements. The difference results from inhomogeneous broadening due to the spatial gradient in the thickness of the cavity layer. For a quality factor of 1500 we expect a width of 0.64 nm, while we measure a width of 1.2 ± 0.1 nm. Because of the focus diameter of $100 \mu\text{m}$ and the spatial gradient of 5.64 nm/mm, we expect a broadening of 0.56 nm. We find a total width of 1.2 ± 0.1 nm if we add the broadening to the unbroadened width. The total width of 1.2 ± 0.1 nm is in perfect agreement with the measured value of 1.2 ± 0.1 nm. The FDTD calculation agrees very well with the measured value and the value obtained from the transfer matrix calculation. No absorption is taken into account in the FDTD calculation, which is the case for the TM model.

The inverse relative linewidth of 830 that we find from the transmission and reflectivity measurements is the result of inhomogeneous broadening of the resonance. The origin of this inhomogeneous broadening is most likely the spatial gradient in the λ -thick GaAs layer. Because there is inhomogeneous broadening, the planar microcavity should be viewed as a static ensemble of microcavities of which each resonance frequency is slightly shifted [16]. This is in agreement with the results presented in [27], where the spatial extent of modes was investigated. The effective radius of the mode is given by $r_{eff}^2 = (Q/2\pi)(\lambda/n)^2$. In our case we find a spatial extent in the order of $5 \mu\text{m}$, which is much smaller than the diameter of the probe beam. In general our results show that the true quality factor of a planar microcavity indeed can only be obtained from a time-resolved measurement.

CONCLUSION

In the case of an inhomogeneously broadened resonance we have shown that the intensity autocorrelate can be used to determine the storage time of a cavity resonance. For an inhomogeneously broadened microcavity resonance we have measured both the spectral width and the intensity autocorrelation trace. The intensity autocorrelation trace yields a value of the quality factor that agrees well with the values found from transfer matrix and FDTD calculations. The spectral width is affected by inhomogeneous broadening and leads to the wrong value for the quality factor.

Acknowledgments

This research was supported by NanoNed, a nanotechnology programme of the Dutch Ministry of Economic Affairs, and by a VICI fellowship from the "Nederlandse Organisatie voor Wetenschappelijk Onderzoek" (NWO) to WLV. This work is also part of the research programme of the "Stichting voor Fundamenteel Onderzoek der Materie" (FOM), which is financially supported by the NWO.

* Electronic address: hartsuiker@amolf.nl

- [1] T. Tanabe, M. Notomi, E. Kuramochi, A. Shinya, and H. Taniyama, Trapping and delaying photons for one nanosecond in an ultrasmall high-Q photonic-crystal nanocavity, *Nat. Phot.* **1**, 49–52 (2007).
- [2] T. Tanabe, M. Notomi, E. Kuramochi, and H. Taniyama, Large pulse delay and small group velocity achieved using ultrahigh-Q photonic crystal nanocavities, *Opt. Express* **15**, 7826–7839 (2007).
- [3] S. F. Preble, Q. Xu, and M. Lipson, Changing the colour of light in a silicon resonator, *Nat. Phot.* **1**, 293–296 (2007).
- [4] J. P. Reithmaier, S. Sek, A. Löffler, C. Hofmann, S. Kuhn, S. Reitzenstein, L. V. Keldysh, V. D. Kulakovskii, T. L. Reinecke, and A. Forchel, Strong coupling in a single quantum dot-semiconductor microcavity system, *Nature* **432**, 197–200 (2004).
- [5] T. Yoshie, A. Scherer, J. Hendrickson, G. Khitrova, H. M. Gibbs, G. Rupper, C. Ell, O. B. Shchekin, and D. G. Deppe, Vacuum Rabi splitting with a single quantum dot in a photonic crystal nanocavity, *Nature* **432**, 200–203 (2004).
- [6] C. Weisbuch, M. Nishioka, A. Ishikawa, and Y. Arakawa, Observation of the coupled exciton-photon mode splitting in a semiconductor quantum microcavity, *Phys. Rev. Lett.* **69**, 3314–3317 (1992).
- [7] J. Kasprzak, M. Richard, S. Kundermann, A. Baas, P. Jeambrun, J. M. J. Keeling, F. M. Marchetti, M. H. Szymanska, R. André, J. L. Staehli, V. Savona, P. B. Littlewood, B. Deveaud, and L. S. Dang, bose-einstein condensation of exciton polaritons, *Nature* **443**, 409 (2006).
- [8] S. Marzenell and R. Beigang, R. and Wallenstein, limitations and guidelines for measuring the spectral width of ultrashort light pulses with a scanning fabry-pérot interferometer, *Appl. Phys. B* **71**, 185–191 (2000).
- [9] F. Erden and O. A. Tretyakov, Excitation by a transient signal of the real-valued electromagnetic fields in a cavity, *Phys. Rev. E* **77**, 056605 (2008).
- [10] R. P. Feynman, R. B. Leighton, and M. Sands, *The Feynman Lectures on Physics Vol. II*, Addison Wesley, 1964.
- [11] J. A. Hart, T. M. Antonsen, Jr., and E. Ott, Scattering a pulse from a chaotic cavity: Transitioning from algebraic to exponential decay, *Phys. Rev. E* **79**, 016208 (2009).
- [12] J. M. Gérard, B. Sermage, B. Gayral, B. Legrand, E. Costard, and V. Thierry-Mieg, Enhanced Spontaneous Emission by Quantum Boxes in a Monolithic Optical Microcavity, *Phys. Rev. Lett.* **81**, 1110–1113 (1998).
- [13] T. Yoshie, J. Vučković, A. Scherer, H. Chen, and D. Deppe, High quality two-dimensional photonic crystal slab cavities, *Appl. Phys. Lett.* **79**, 4289 (2001).
- [14] T. Asano, B.-S. Song, and S. Noda, Analysis of the experimental Q factors (~ 1 million) of photonic crystal nanocavities, *Opt. Express* **14**, 1996–2002 (2006).
- [15] P. J. Harding, T. G. Euser, Y. R. Nowicki-Bringuier, J.-M. Gérard, and W. L. Vos, Ultrafast optical switching of planar GaAs/AlAs photonic microcavities, *Appl. Phys. Lett.* **91**, 111103 (2007).
- [16] A. Lagendijk, *Vibrational relaxation studied with light*, in: *Ultrashort Processes in Condensed Matter*, Edited by W. E. Bron, Plenum, New York, 1993.
- [17] W. Demtröder, *Laser Spektroskopie*, 1996.
- [18] D. K. Armani, T. J. Kippenberg, S. M. Spillane, and K. J. Vahala, Ultra-high-Q toroid microcavity on a chip, *Nature* **421**, 925–928 (2003).
- [19] J.-C. Diels and W. Rudolph, *Ultrashort Laser Pulse Phenomena: Fundamentals, Techniques, and Applications on a Femtosecond Time Scale*, Academic press, Burlington, 2 edition, 1996.
- [20] J. M. Gérard, D. Barrier, J. Y. Marzin, and T. Rivera, Quantum boxes as active probes for photonic microstructures: The pillar microcavity case, *Appl. Phys. Lett.* **69**, 449–451 (1996).
- [21] P. Harding, *Photonic Crystals Modified by Optically Resonant Systems*, PhD thesis, 2008.
- [22] M. S. Thijssen, R. Sprik, J. E. G. J. Wijnhoven, M. Megens, T. Narayanan, A. Lagendijk, and W. L. Vos, Inhibited Light Propagation and Broadband Reflection in Photonic Air-Sphere Crystals, *Phys. Rev. Lett.* **83**, 2730–2733 (1999).
- [23] A. Farjadpour, J. D. Joannopoulos, S. G. Johnson, and G. Burr, improving accuracy by subpixel smoothing in FDTD, *Opt. Lett.* **31**, 2972–2974 (2006).
- [24] J. S. Blakemore, Semiconducting and other major properties of gallium arsenide, *J. Appl. Phys.* **53**, R123–R181 (1982).
- [25] R. E. Fern and A. Onton, Refractive Index of AlAs, *J. Appl. Phys.* **42**, 3499–3500 (1971).
- [26] B. E. A. Saleh and M. C. Teich, *Fundamentals of photonics*, Wiley Interscience, New York, 1991.
- [27] F. de Martini, M. Marrocco, and D. Murra, Transverse quantum correlations in the active microscopic cavity, *Phys. Rev. Lett.* **65**, 1853–1856 (1990).
- [28] The maximum unbroadened refractive index change of the dots amounts to only 10^{-8} , while the absorption at resonance is less than 0.02 cm^{-1} .
- [29] We used $e^{-t\omega_0/Q}$ as the impulse response of intensity in the cavity.